Applied Acoustics 72 (2011) 754–759

Contents lists available at ScienceDirect

Applied Acoustics

journal homepage: www.elsevier.com/locate/apacoust

Acoustic force model for the fluid flow under standing waves

Hong Lei [a,b,*], Daniel Henry [a], Hamda BenHadid [a]

[a] Laboratoire de Mecanique des Fluides et d'Acoustique, UMR CNRS 5509, Ecole Centrale de Lyon/Universite Claude Bernard Lyon 1/INSA de Lyon, ECL, 36 Avenue Guy de Collongue, 69134 Ecully Cedex, France

[b] Key Laboratory of Electromagnetic Processing of Materials, Ministry of Education, Northeastern University, Shenyang 110819, China

ARTICLE INFO

Article history:
Received 15 December 2009
Received in revised form 4 September 2010
Accepted 18 April 2011
Available online 11 May 2011

Keywords:
Acoustic streaming
Standing wave
Acoustic boundary layer
Mathematical model

ABSTRACT

An acoustic Strouhal number is introduced to demonstrate that the viscosity of fluid can be ignored in the process of sound propagation and acoustic streaming is independent on the frequency of the acoustic wave. Furthermore, acoustic force based on the periodic velocity fluctuation caused by standing acoustic wave is introduced into Navier–Stokes equation in order to describe the fluid flow in the acoustic boundary layer. The numerical results show that the predicted results are consistent with the analytic solution. And the effect of the nonlinear terms cannot be ignored so the analytic solution derived by boundary-velocity condition is only an approximation for acoustic streaming.

1. Introduction

It is well known that sound wave propagation through the fluid can form steady vortex flow near the wall. Such a steady flow is due to the interaction between the inertia and viscosity forces, but the magnitude of the velocity is independent of the viscosity [1,2]. Rayleigh [1] and Westervelt [3] gave the profile of streaming velocity between two parallel planes. Further, Vainshtein [4,5] and Lei et al. [6] studied the effect of standing waves on the heat transfer. But it should be pointed out that the quadratic terms are neglected and the thickness of the acoustic boundary layer is assumed to be zero in their models. Because there is the velocity fluctuation caused by the sound field, the turbulence theory can be applied to calculate acoustic streaming. But the effects of the unsteady term and the acoustic boundary layer are not considered in the previous work [7,8]. Therefore, on the base of the turbulence theory and the non-steady boundary-layer theory, we propose a new mathematical model to predict acoustic streaming. And such a model can describe the fluid flow in the acoustic boundary layer.

In the rest of this paper, we make some assumptions and analyze the rationality of these assumptions (Section 2.1–2.2). Based on the ideas of the Reynolds averaged Navier–Stokes model, we propose the acoustic force model and interpret the physical meaning of the acoustic streaming number (Section 2.3–2.5). Finally, we perform numerical computation and compare the predicted result with an analytic solution derived by the boundary-velocity condition (Section 3).

2. Acoustic force model

2.1. Assumptions

The current mathematical model are derived on the base of the following assumptions:

(1) The sound propagates in the fluid as the form of plane waves.
(2) The sound speed is far greater than the fluid velocity, so the period for the compression and expansion of the fluid is much smaller than that for the heat transfer. In other words, it is an adiabatic process.
(3) During the process of sound propagation in the fluid, the viscosity effect may be neglected.
(4) During the process of sound propagation in the fluid, the pressure fluctuation is very small relative to the mean pressure, so sound propagation may be studied by the linearized equations.
(5) The fluid flow is independent of the frequency of the acoustic wave.

2.2. Acoustic Strouhal number

In order to characterize the fluid dynamic response to the sound wave, we introduce the acoustic Strouhal number

* Corresponding author at: Laboratory of Electromagnetic Processing of Materials, Ministry of Education, Northeastern University, Shenyang, 110819, China
E-mail address: cn_leihong@yahoo.com (H. Lei).

0003-682X/$ - see front matter © 2011 Elsevier Ltd. All rights reserved.
doi:10.1016/j.apacoust.2011.04.007

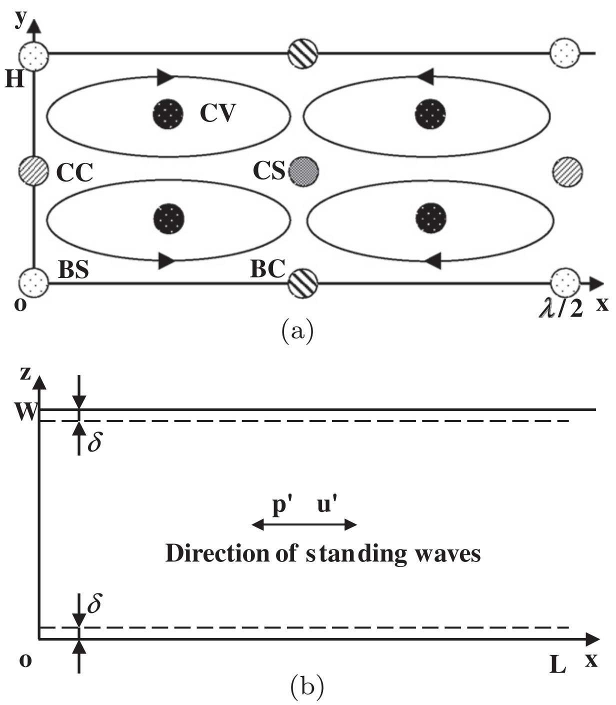

Fig. 1. Acoustic streaming in a rectangular pipe. (a) Front view. (b) Top view.

$$S_t = \frac{T_d}{T_a} = \frac{fH^2}{v} \tag{1}$$

Here T_a and f are the period and the frequency of the acoustic waves, respectively. And T_d is the characteristic time of momentum diffusivity which can be defined as follows:

$$T_d = H^2/v \tag{2}$$

where v is the fluid kinematic viscosity.

If the plane acoustic wave propagates along the x direction in the rectangular pipe [9] shown in Fig. 1, the height H and width W of the pipe should satisfy

$$\max\{W, H\} < \frac{\lambda}{2} \tag{3}$$

where λ is the wavelength.

Eliminating the height of the pipe in virtue of the plane acoustic wave condition (3), we obtain

$$S_t < S_t^* = \frac{c_0^2}{4fv} \tag{4}$$

Here c_0 is the speed of the sound in the fluid. And the critical acoustic Strouhal number S_t^* may be regarded as an approximation for Eq. (1).

In most cases, the height of the pipe is about $\lambda/10$, and it is easy to satisfy $S_t \gg 1$ for water and air according to Table 1 [10–12]. Thus, the characteristic time of momentum diffusivity is usually much longer than the period of the acoustic wave, i.e. the slow flow of the fluid cannot follow the variation of acoustic field (assumption 5). In other words, the viscosity can be neglected during the sound wave propagation through the fluid (assumption 3).

2.3. Standing wave

Let us consider the acoustic streaming on the condition of standing waves in an infinite pipe. The geometry and coordinate systems are shown in Fig. 1. The vortical structures in pairs can be observed in the planes xoy and xoz if the standing wave is applied at the x direction.

Table 1
Physical parameters and critical Strouhal number in the acoustic streaming.

	c_0 (m/s)	v (m^2/s)	f (kHz)	S_t^*	S_t ($H = \lambda/10$)
Air (20 °C)	344	15.6×10^{-6}	2	9.5×10^5	3.8×10^4
Water (20 °C)	1483	1.0×10^{-6}	20	2.7×10^7	1.1×10^6

In this case, the velocity fluctuation u' may be written as

$$u' = -u_1 \sin kx \cos \omega t \tag{5}$$

with

$$u_1 = \frac{p_1}{\rho_0 c_0} \tag{6}$$

where the density of the fluid ρ_0 is a constant, ω is the angular frequency, $k = \frac{\omega}{c_0}$ is the wave number, and p_1 is the amplitude of the acoustic pressure fluctuation p'. Here, the subscript "1" in Eq. (5) indicates the amplitude of the quantity fluctuation.

According to the analytic solution for the boundary layer near an oscillating flat plate [2], the velocity fluctuation in the pipe can be written in a general way as:

$$u' = -u_1 \sin kx \left[\cos \omega t - \tilde{\psi}_y - \tilde{\psi}_z\right] \tag{7}$$

where the quantities $\tilde{\psi}_y$ and $\tilde{\psi}_z$ are the functions of y and z.

$$\tilde{\psi}_y = \begin{cases} 0 & \eta \geqslant 1 \\ e^{-\frac{\pi}{2}\eta} \cos\left(\omega t - \frac{\pi}{2}\eta\right) & \eta < 1 \end{cases} \tag{8}$$

$$\tilde{\psi}_z = \begin{cases} 0 & \zeta \geqslant 1 \\ e^{-\frac{\pi}{2}\zeta} \cos\left(\omega t - \frac{\pi}{2}\zeta\right) & \zeta < 1 \end{cases} \tag{9}$$

with

$$\eta = \frac{y}{\delta} \tag{10}$$

$$\zeta = \frac{z}{\delta} \tag{11}$$

$$\delta = \frac{\pi}{2}\sqrt{\frac{2v}{\omega}} \tag{12}$$

2.4. Acoustic force

In most cases, the fluid velocity consists of the time-averaged velocity and the fluctuating velocity. The frequency of the fluctuating velocity is too high to be of much interest, so we shall confine ourselves to the time-averaged flow. One of the most famous examples is the Reynolds Averaged Navier–Stokes (RANS) equations, which are widely applied to describe the incompressible turbulent flow [13].

$$\frac{\partial V_i}{\partial x_i} = 0 \tag{13}$$

$$\rho V_j \frac{\partial V_i}{\partial x_j} = -\frac{\partial p}{\partial x_i} + \frac{\partial}{\partial x_j}\left(\rho v \frac{\partial V_i}{\partial x_j} + \tau_{i,j}\right) \tag{14}$$

where $\tau_{i,j} = -\rho\overline{V_i' V_j'}$ $(i, j = 1, 2, 3)$ is Reynolds stress tensor. The force per unit volume, F_i, which is caused by the spatial variation of the Reynolds stress, can be expressed as

$$F_i = -\frac{\partial\left(\rho\overline{V_i' V_j'}\right)}{\partial x_j} \tag{15}$$

Provided that the velocity fluctuation V' is caused by the sound field and the velocity fluctuation occurs in the direction of sound propagation, we may obtain a similar force term according to the acoustic velocity u' profile.

$$F_i = \begin{cases} -\rho_0\overline{u'\frac{du'}{dx}} - \overline{\rho'\frac{\partial u'}{\partial t}} = -\frac{1}{T_a}\int_0^{T_a}\left(\rho_0 u'\frac{du'}{dx} + \rho'\frac{\partial u'}{\partial t}\right)dt & (i=1) \\ 0 & (i=2,3) \end{cases} \quad (16)$$

where ρ' is the density fluctuation.

$$\rho' = -\rho_0\int_0^t \frac{\partial u'}{\partial x}d\tilde{t} = -\rho_1\cos kx\sin\omega t \quad (17)$$

Here $\rho_1 = -\frac{p_1}{c_0^2}$ is the amplitude of density fluctuation.

Taking the effect of the boundary layer into account, Eq. (17) becomes

$$\rho' = -\rho_1\cos kx[\sin\omega t - \tilde{\phi}_y - \tilde{\phi}_z] \quad (18)$$

where $\tilde{\phi}_y$ and $\tilde{\phi}_z$ are the functions of y and z.

$$\tilde{\phi}_y = \begin{cases} 0 & \eta \geqslant 1 \\ e^{-\frac{\pi}{2}\eta}\sin(\omega t - \frac{\pi}{2}\eta) & \eta < 1 \end{cases} \quad (19)$$

$$\tilde{\phi}_z = \begin{cases} 0 & \zeta \geqslant 1 \\ e^{-\frac{\pi}{2}\zeta}\sin\left(\omega t - \frac{\pi}{2}\zeta\right) & \zeta < 1 \end{cases} \quad (20)$$

Substituting the velocity fluctuation equation (7) and the density fluctuation equation (18) into Eq. (16), the non-zero component of acoustic force representing the effects of acoustic waves on the fluid flow becomes

$$F_x = -\frac{\pi C_{As}\rho_0 u_1^2}{\lambda}\sin 2kx \quad (21)$$

with

$$C_{AS} = 1 - 2\psi_y - 2\psi_z + 2\psi_y\psi_z + 2\phi_y\phi_z + \varphi_y^2 + \varphi_z^2 \quad (22)$$

$$\psi_y = \begin{cases} 0 & \eta \geqslant 1 \\ e^{-\frac{\pi}{2}\eta}\cos\frac{\pi}{2}\eta & \eta < 1 \end{cases} \quad (23)$$

$$\psi_z = \begin{cases} 0 & \zeta \geqslant 1 \\ e^{-\frac{\pi}{2}\zeta}\cos\frac{\pi}{2}\zeta & \zeta < 1 \end{cases} \quad (24)$$

$$\phi_y = \begin{cases} 0 & \eta \geqslant 1 \\ e^{-\frac{\pi}{2}\eta}\sin\frac{\pi}{2}\eta & \eta < 1 \end{cases} \quad (25)$$

$$\phi_z = \begin{cases} 0 & \zeta \geqslant 1 \\ e^{-\frac{\pi}{2}\zeta}\sin\frac{\pi}{2}\zeta & \zeta < 1 \end{cases} \quad (26)$$

$$\varphi_y = \begin{cases} 0 & \eta \geqslant 1 \\ e^{-\frac{\pi}{2}\eta} & \eta < 1 \end{cases} \quad (27)$$

$$\varphi_z = \begin{cases} 0 & \zeta \geqslant 1 \\ e^{-\frac{\pi}{2}\zeta} & \zeta < 1 \end{cases} \quad (28)$$

2.5. Acoustic streaming

We introduce non-dimensional variables with the help of the following scales: H for length, H^2/ν for time, ν/H for velocity, and define the acoustic streaming number.

$$As = \frac{\pi u_1^2 H^3}{\lambda\nu^2} \quad (29)$$

The non-dimensional governing equations can be rewritten as follows:

$$\nabla\cdot\vec{V^*} = 0 \quad (30)$$

$$\frac{\partial\vec{V^*}}{\partial t^*} + (\vec{V^*}\cdot\nabla)\vec{V^*} = -\nabla p^* + \nabla^2\vec{V^*} + AsC_{AS}\sin\left(4\pi x^*\frac{H}{\lambda}\right)\vec{e}_x \quad (31)$$

where the asterisk physical variables are the dimensionless variables.

The acoustic streaming number, which has an explicit physical meaning, may be expressed as follows.

$$As = \frac{\pi^3}{2}\left(\frac{\rho_1}{\rho_0}\right)^2\left(\frac{c_0\lambda}{2\pi\nu}\right)^2\left(\frac{2H}{\lambda}\right)^3 \quad (32)$$

It is composed of four parts. The first part $\pi^3/2$ is the constant term. The second part ρ_1/ρ_0 denotes the amplitude of the density fluctuation or the amplitude of the acoustic pressure. The third part $\frac{c_0\lambda}{2\pi\nu} = \frac{K_s}{\omega\rho\nu}$ represents the ratio of the elastic force to the viscous force [9], where K_s is the bulk modulus in units of pressure. And the third part can be rewritten as follows:

$$\frac{c_0\lambda}{2\pi\nu} = \frac{\pi}{2}S_t^* \quad (33)$$

Table 1 shows that S_t is in the order 10^4–10^6 so the third part is far greater than unity. The last part is related to the plane acoustic wave condition equation (3), which is less than unity.

2.6. Boundary conditions and solution method

The boundary conditions are expressed as follows:

(1) At the wall, the velocity is equal to zero and the normal gradient of the pressure is prescribed as zero.
(2) At the inlet and outlet, the periodic condition is applied for all the variables.

The governing equations for acoustic force model consists of Eqs. (22) and (32). An in-house code is developed to solve the partial differential equations on a staggered-point grid. The calculational domain is discretized by using a nonuniform grid with a densely packed grid in the acoustic boundary layer. The pressure and the acoustic force are evaluated at the grid node while the velocity components were defined at the interface between the grid nodes. The central-difference scheme and upwind scheme are applied to treat the diffusion term and the convection term, respectively. The pressure–velocity coupling is handled by using the SIMPLE (Semi-Implicit Method for Pressure-Linked Equations) algorithm [14]. And the discretized equations are solved by using the tri-diagonal matrix algorithm coupled with the Gauss–Seidel routine.

The convergence criteria is expressed as follows:

$$\left|\frac{\vec{V}^{(K+1)} - \vec{V}^{(K)}}{\vec{V}^{(K+1)}}\right| < 10^{-9} \quad (34)$$

where K is the iteration number.

3. Results and discussion

3.1. Model experiment

The experimental condition of Arroyo and Greated [11] was employed to verify the present mathematic model. The experimental conditions for the calculation are summarized as: the sizes of the calculation domain are $L = \frac{\lambda}{2}$ and $L:H = 4.056:1$, respectively. The ratio of the thickness of the boundary layer to the height is $\delta:H = 1:277.18$, and the acoustic streaming number is $As = 1.815 \times 10^6$.

Table 2
Tests of numerical accuracy with different meshes.

	41 × 201	51 × 241	61 × 281	71 × 301	81 × 321
Nodes in the boundary layer	58	64	77	90	96
u_{max}	3.111260	3.107508	3.116109	3.102976	3.105022
v_{max}	0.455731	0.454902	0.456254	0.453942	0.455320
$u_{max}(y=\frac{H}{2})$	1.482344	1.479444	1.486439	1.478086	1.480441

3.2. Analytic solution

According to the boundary-layer theory [1], there is a steady velocity outside the acoustic boundary. Its magnitude is

$$u_0 = \frac{3u_1^2}{8c_0}\sin 2kx \tag{35}$$

The acoustic layer is so thin that it can be assumed to be zero, so the steady velocity can be served as a boundary condition to determine the acoustic streaming. Such a boundary condition is called as the boundary-velocity condition [6].

Since u_1 is assumed to be infinitesimal, the quadratic terms in Navier–Stokes equation may be neglected. Moreover, the derivatives with respect to y are much larger than that with respect to x on the base of $H \ll \lambda$. Neglecting the latter and using the boundary-velocity condition, the velocity distribution can be describe as [4]

$$V_x = -\frac{3u_1^2\sin 2kx}{16c_0}\left[1 - \frac{3(y-H/2)^2}{(H/2)^2}\right] \tag{36}$$

$$V_y = \frac{3ku_1^2\cos 2kx}{8c_0}\left[\left(y - \frac{H}{2}\right) - \frac{(y-H/2)^3}{(H/2)^2}\right] \tag{37}$$

Consequently, according to the above experimental conditions, the non-dimensional horizontal velocity at the central line is $u^* = 1.795 \sin(4\pi x^* H/\lambda)$.

3.3. Computational grid and numerical results

Special attention is paid to the construction of the computational grid. The boundary layer is so thin that there is the greater gradient of the fluid velocity there, so many grid nodes should be applied in the thin acoustic boundary layer. In this paper, we use more than 50 uniform grids inside the acoustic boundary layer, and nonuniform grids outside the acoustic boundary layer.

To ensure that the solutions are not spurious artifacts of poorly resolved grids, grid sensitivity experiments have been carried out in different meshes. Table 2 gives the maxima of the velocity obtained on the grid nodes for five different meshes. When the grid is refined from 41 × 201 to 81 × 321, the maxima of the velocity components agree within 0.51%. Between the meshes from 71 × 301 to 81 × 321, the variation of u_{max} is on the third digit, the difference on v_{max} is 0.001378, i.e. approximately 0.3%. Considering the fact that the maximum value is not always on the points of the mesh, u_{max} and v_{max} cannot be absolutely the same by using different meshes. In present paper, the 81 × 321 mesh is sufficiently fine to resolve the acoustic streaming.

Fig. 2 shows the numerical solution by acoustic force model is similar to the analytic solution. Standing waves applied in the fluid at rest can form the time-averaged fluid flow, which has arrays of large-scale, spanwise, counter-rotating vortical structures. The velocity increases rapidly from zero at the wall to the maximum at the thickness of the acoustic layer and decreases slowly with the further increase of the distance from the wall. Some stagnation points are located at equally spaced intervals. A more distinct picture about the stagnation points may be found in Fig. 1a. One of these points is "CV", the center of the vortex. The points("BC" and "BS") on the wall are generated by the combination and sepa-

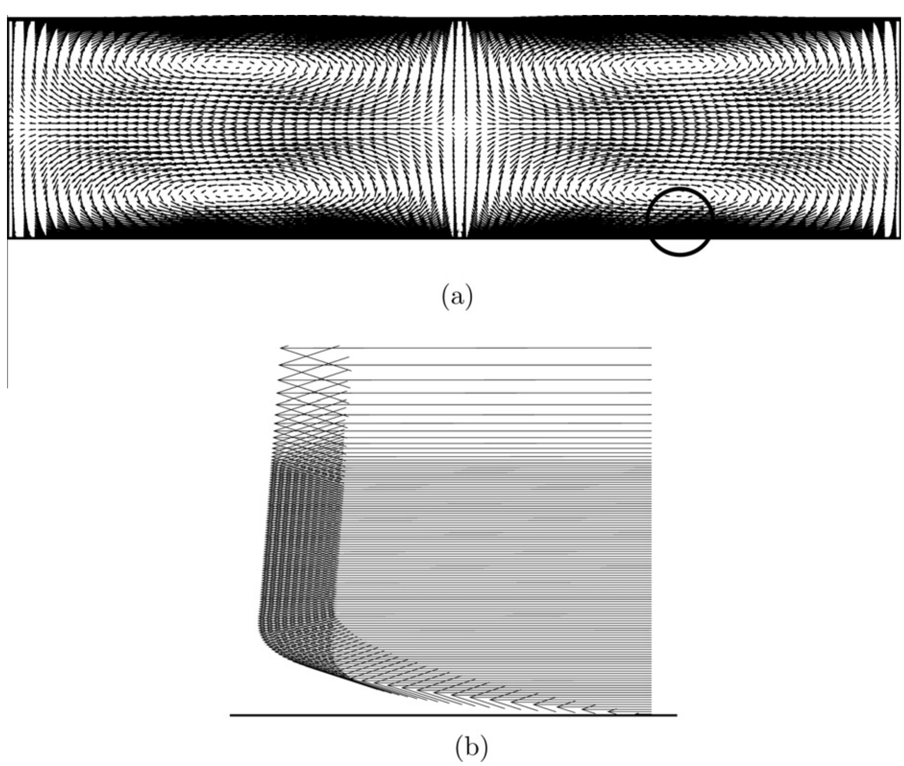

Fig. 2. Predicted flow field under standing waves. (a) Acoustic streaming. (b) Enlarged picture.

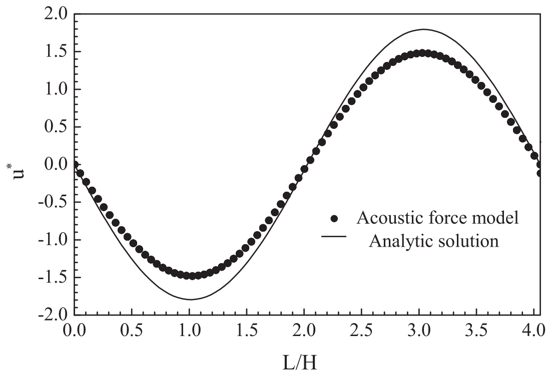

Fig. 3. Fluid velocity at central line.

ration of the stream in the boundary layer. The others (“CC” and “CS”) are generated by the combination and separation of the return flow at the central line.

3.4. Model validity

The maxima of the horizontal velocity at the central line is about 47.7% of that in the calculation domain, as shown in Table 2. It is close to 50% predicted by analytic solution. But Fig. 3 shows the relative difference for $u_{max}(y = H/2)$ between the acoustic force model and analytic solution is 17.5%. Such a difference comes from two assumptions in analytic solution. (1) The wavelength should be far greater than the characteristic length of the pipe, $\lambda \gg H$. But in the current case, $H/\lambda = 1:8.112$. (2) The quadratic terms could be neglected since the velocity of the steady flow is a small quantity with respect to the sound speed. But such an assumption is not valid near the wall. In order to estimate the effect of quadratic terms, it is necessary to calculate the Reynolds numbers, *Rex* and *Rey*.

$$Rex = \left| \frac{\rho u \frac{\partial u}{\partial x} + \rho v \frac{\partial u}{\partial y}}{\mu \frac{\partial^2 u}{\partial x^2} + \mu \frac{\partial^2 u}{\partial y^2}} \right| \tag{38}$$

$$Rey = \left| \frac{\rho u \frac{\partial v}{\partial x} + \rho v \frac{\partial v}{\partial y}}{\mu \frac{\partial^2 v}{\partial x^2} + \mu \frac{\partial^2 v}{\partial y^2}} \right| \tag{39}$$

Fig. 4a and b gives the relative magnitude of the quadratic terms. For *u*, the effects of the nonlinear terms cannot be ignored near the wall and near the “CS” point because of $Rex > 0.2$ in these regions. For *v*, the quadratic terms play a greater role. The region for $Rey > 0.2$ is larger than that for $Rex > 0.2$. It is especially to be remarked that *Rey* is greater than 1.0 in the regions among the points “CC”, “CS” and “CV” and the regions near the midpoint between “BC” and “BS”. In that way, the nonlinear terms are more important than the linear terms. The facts that $Rex > 0.2$ and $Rey > 0.2$ occur in some regions indicate that the analytic solution cannot exactly describe the acoustic streaming in the pipe.

3.5. Fluid viscosity

Acoustic streaming is induced by attentuation of acoustic waves. The fluid viscosity is one of attentuation mechanisms. Acoustic streaming involves in the oscillation flow and the steady flow.

(1) The oscillation flow has direct relation to the sound propagation. The fluid viscosity should be considered in the case of the sound propagation in the boundary layer [2], but it can be ignored in the case of the sound propagation outside the boundary layer.
(2) The steady flow in the boundary layer is the result of interaction between the acoustic force and the viscous force. Further, the steady vortices structure outside the boundary layer also comes from the fluid viscosity [4]. Fig. 4 shows the effect of the fluid viscosity is larger than(is not much larger than) that of the inertia near the wall, so it is better to consider the effect of nonlinear terms.

3.6. Acoustic streaming number

The Acoustic streaming number is a dimensionless number that gives a measure of the ratio of acoustic force to viscous force, and has a similar form of Reynolds number.

$$As = \frac{\pi H}{\lambda} \left(\frac{u_1 H}{\nu} \right)^2 \tag{40}$$

Acoustic streaming occurs at higher acoustic streaming number and is dominated by the acoustic force. If the acoustic streaming number is very low, no acoustic streaming occurs.

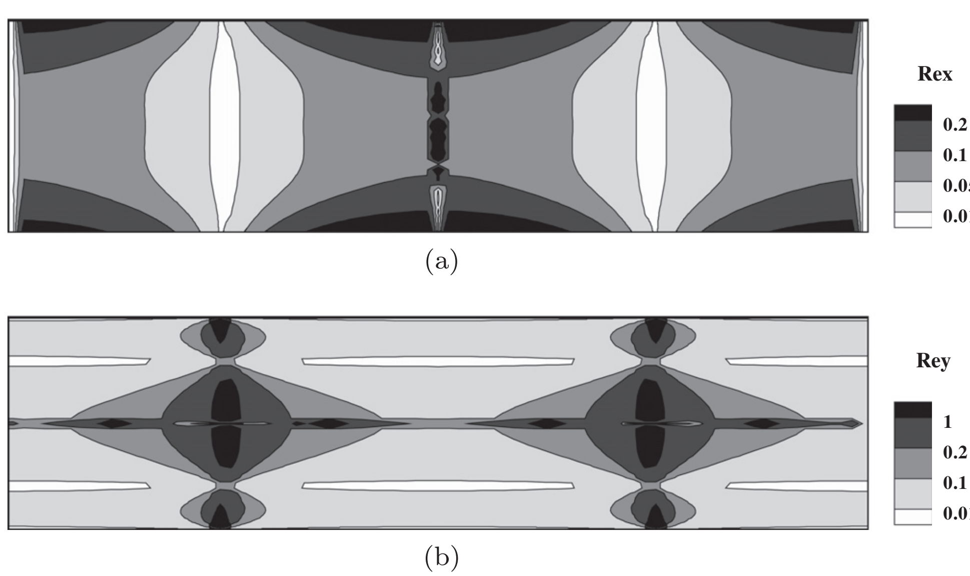

Fig. 4. Reynolds number predicted by the acoustic force model. (a) Rex. (b) Rey.

4. Conclusion

(1) In virtue of the idea of the Reynolds averaged Navier–Stokes equations, a mathematic model is developed to describe the fluid flow in the acoustic boundary layer and outside the boundary layer. And the predicted fluid flow outside the boundary layer is similar to the analytic solution.

(2) Acoustic Strouhal number is introduced to demonstrate the fluid can be treated as the inviscid fluid during the sound propagation and the fluid flow is independent of the frequency of the acoustic wave.

(3) Numerical result of Reynolds number shows that the viscosity play an important role in the acoustic streaming, and the nonlinear terms in the Navier–Stokes equations cannot be ignored in order to calculate acoustic streaming exactly.

Acknowledgments

The authors would like to thank the Institut du developpement et des ressources en informatique scientifique, SRF for ROCS, SEM (20071108-2) and NEU, the Fundamental Research Funds for the Central Universities (N100409007).

References

[1] Rayleigh Baron JWS. The theory of sound, 2nd ed., vol. 2. New York: Dover Publications; 1945.
[2] Schlichting H. Boundary-layer theory. 7th ed. New York: McGraw-Hill; 1979.
[3] Westervelt PJ. The theory of steady rotational flow generated by a sound field. J Acoust Soc Am 1953;25(1):60–7.
[4] Vainshtein P, Fichman M, Gutfinger C. Acoustic enhancement of heat transfer between two parallel plates. Int J Heat Mass Transfer 1995;38(10):1893–9.
[5] Vainshtein P, Gutfinger C, Pnueli D. Ignition of fuel mixtures by standing acoustic waves. Combust Flame 1999;118(3):370–80.
[6] Lei H, Henry D, BenHadid H. Numerical study of the influence of a longitudinal sound field on natural convection in a cavity. Int J Heat Mass Transfer 2006;49(19-20):3601–16.
[7] Lighthill J. Acoustic streaming. J Sound Vib 1978;61(3):391–418.
[8] Valdes LC, Santens D. Influence of permanent turbulent air flow on acoustic streaming. J Sound Vib 2000;230(1):1–29.
[9] Du GH, Zhu ZM, Gong XF. Basic acoustics. 2nd ed. Nanjing (China): Nanjing University Publication; 2001.
[10] Vainshtein P, Fichman M, Shuster K, Gutfinger C. The effect of centreline particle concentration in a wave tube. J Fluid Mech 1996;306:31–42.
[11] Arroyo MP, Greated CA. Stereoscopic particle image velocimetry. Meas Sci Technol 1991;2(12):1181–6.
[12] Campbell M, Cosgrove JA, Greated CA, Jack S, Rockliff D. Review of LDA and PIV applied to the measurement of sound and acoustic streaming. Opt Laser Technol 2000;32(7-8):629–39.
[13] Ferziger JH, Peric M. Computational methods for fluid dynamics. New York: Springer-Verlag; 1996.
[14] Patankar SV. Numerical heat transfer and fluid flow. Washington: Hemisphere Publishing Corporation; 1980.